Regulatory Peptides 177 (2012) 97–106

Contents lists available at SciVerse ScienceDirect

Regulatory Peptides

journal homepage: www.elsevier.com/locate/regpep

Effects of maternal captopril treatment during late pregnancy on neonatal lung development in rats

Diego N. Capelari [a,b], Susana I. Sánchez [b], Hugo H. Ortega [c], Gladys M. Ciuffo [a], Lucia B. Fuentes [b,*]

[a] Instituto Multidisciplinario de Investigaciones Biológicas (IMIBIO-SL), Consejo Nacional de Investigaciones Científicas y Tecnológicas (CONICET), Argentina
[b] Facultad de Química, Bioquímica y Farmacia, Universidad Nacional de San Luis (UNSL), Ejército de los Andes 950, D5700HHW San Luis, Argentina
[c] Departamento de Ciencias Morfológicas, Facultad de Ciencias Veterinarias, Universidad Nacional del Litoral (UNL), R.P. Kreder 2805, S3080HOF Esperanza, Santa Fe, Argentina

ARTICLE INFO

Article history:
Received 21 October 2011
Received in revised form 10 March 2012
Accepted 5 May 2012
Available online 12 May 2012

Keywords:
Renin angiotensin system
Angiotensin-converting enzyme
Captopril
Postnatal lung development
Cellular proliferation
Pulmonary dysplasia

ABSTRACT

The renin–angiotensin system (RAS) has been implicated in pulmonary hypertension and pulmonary fibrosis. In the present study, we examined the effects of maternal exposure to captopril (2.85 mg/kg/day) during late pregnancy (G13–G21) on postnatal rat lung development. Treatment with captopril during late pregnancy caused a significant decrease in ACE activity in P0 rats. Body weight decreased at P0 ($p<0.001$), P8 and P15 ($p<0.01$) in captopril-treated rats. Lung weight of P0 and P8 pups was lower in treated-animals ($p<0.05$). Lungs from captopril-treated animals showed impaired alveolar formation, with enlarged distal airway spaces at P8, P15 and P30. Interalveolar wall distance measured by mean linear intercept increased in treated vs. age-matched animals at P8, P15 ($p<0.001$) and P30 ($p<0.05$) resembling new bronchopulmonary dysplasia. In control animals, the proliferating cell nuclear antigen (PCNA) marker was higher at P0 and then drops gradually, while in captopril-treated animals PCNA marker remains higher at all stages studied. α-Smooth muscle actin (α-SMA), a marker of fibroblast differentiation into myofibroblasts, was higher at the tips of developing secondary septa in captopril-treated lungs at P8 and P15. The increased expression of PCNA and α-SMA in treated pups suggest that beyond the effect caused by captopril, the developing lungs have the capacity to recover once the treatment was stopped. Taking together the low weight, histomorphological changes and increased expression of cellular markers caused by ACE inhibition during late pregnancy, it appears that the RAS could be an intrinsic factor involved in secondary septa formation during lung development.

1. Introduction

Angiotensin II (Ang II), the active peptide of the renin–angiotensin system (RAS), plays a key role in blood pressure regulation, and body fluid and electrolyte homeostasis [1,2]. Besides, Ang II has been recognized as a growth factor, either by itself or through interactions with other growth factors [2–5]. Ang II effects are mediated by interaction with specific receptors which have been pharmacologically classified in two subtypes, designated as AT_1 and AT_2 [1].

Angiotensin converting enzyme (ACE, E.C. 3.4.15.1), is a Zn^{2+} metallopeptidase member of the RAS, responsible for proteolytic cleavage of Ang I into Ang II [6]. The ACE gene codifies for two splice variants, the somatic isoform (sACE) expressed primarily in endothelial and epithelial cells, and the testicular isoform [7]. The discovery of ACE inhibitors represents a major advance in treatment of hypertension, being captopril the first one developed [8]. Captopril has been often used during pregnancy and adverse birth outcomes have been reported. Captopril exposures during pregnancy have been associated with pre- and postnatal developmental disorders, such as oligohydramnios, intrauterine growth restriction, congenital malformations secondary to oligohydramnios (retarded ossification of skull bones, limb positional deformities), fetal renal tubular pathology, neonatal renal failure, pulmonary hypoplasia and early postnatal death [8–10].

Studies from the ontogeny, knock-out mice and blockade of the RAS provide strong evidence about the role of the RAS during development of different organs [3–5,11–13]. The RAS has been implicated in pulmonary hypertension and pulmonary fibrosis and plays a critical role in chronic and acute lung diseases, particularly in acute respiratory distress syndrome [14–16]. Nogueira-Silva et al. recently demonstrated that all RAS components were constitutively expressed in the rat lung during gestation (G15 to G21) and that Ang II had a stimulatory effect on lung branching, mediated by AT_1 receptors [12].

ACE inhibitors have the ability to pass the fetoplacental barrier [17,18]. Thus, the use of these inhibitors during pregnancy is contraindicated because of increased risks of fetopathy including malformations of the cardiovascular, renal, and central nervous systems [8–10,18,19]. However, very little information is available regarding

* Corresponding author.
E-mail address: lfuen@unsl.edu.ar (L.B. Fuentes).

0167-0115/$ – see front matter © 2012 Elsevier B.V. All rights reserved.
doi:10.1016/j.regpep.2012.05.092

damage on the developing lung of offsprings born from pregnant rats treated with ACE inhibitors [8–10]. Although a number of knock-out mice have been developed, the major defects reported were blood pressure reduction, renal pathology and reduced fertility, but no data were provided with reference to lung development [13].

The formation of definitive alveoli by secondary septation of large saccules that constitute the gas-exchange region of immature lung, begins during late gestation and continues postnatally [20]. Secondary septa form as ridges that grow into distal air spaces, increasing lung surface and gas exchange capacity [21]. Rat lung alveolarization begins during late gestation and continues on the first 2–3 postnatal weeks [21] being sensitive to perinatal treatments [22–24].

Bronchopulmonary dysplasia (BPD) and emphysema are both characterized by deficit in alveolar number and increased airspace size, leading to reduction of the exchange-surface-to-volume ratio and respiratory insufficiency. BPD is commonly observed postnatally in very low birth weight premature neonates, while emphysema is observed in adults [25,26].

The role of RAS during lung development and functional differentiation is not clearly established. In the lung, ACE activity and expression begins from gestational day 15 (G15) until adulthood [27,28]. Early postnatal ACE inhibition caused increase of alveolar surfactant, wider respiratory airspaces and thinner alveolar septa in enalapril-treated rats [24]. Although ACE is highly expressed in developing lungs and has a potentially important physiological role, the effect of ACE inhibitors administered during late pregnancy has not been extensively studied. In order to evaluate the potential role of the RAS during lung development, we designed an experimental model of treatment of the mother without drastic teratogenic effects, allowing us to evaluate the participation of the RAS in the development. Thus, clinical or subclinical doses were used and morphogenesis, alveolarization and proliferation were evaluated on neonatal lung development.

2. Materials and methods

2.1. Animal treatment

Pregnant Wistar rats (230–250 g) were kept in a dark–light cycle (12:12 h, at 22 ± 1 °C) and fed with standard rodent food and water ad libitum. On the 13th day of pregnancy (G13), they were randomly assigned to two experimental groups: control ($n = 6$) and captopril-treated ($n = 6$) rats. Mini-osmotic pumps (Alzet model 2001; Palo Alto, CA) were implanted subcutaneously between the scapulae bones under light ether anesthesia [4,5], containing sterile isotonic saline solution (control), or captopril (2.85 mg/kg/day) [(2S)-N-(3-mercapto-2-methylpropionyl)-L-proline] (C-4042, Sigma-Aldrich, USA). The in vivo effects of prenatal exposure to captopril were evaluated in lungs from different postnatal ages: 0 (P0), 8 (P8), 15 (P15) and 30 (P30) days. Thus, histological and morphometrical analyses of lungs, alveolarization and proliferation of alveolar cells were evaluated. Moreover, the expression of somatic ACE, AT_1 and AT_2 receptors was determined.

The Local Ethical Committee of the Universidad Nacional de San Luis approved all animal experimentation. Animals were handled in accordance with the Guide for the Care and Use of Laboratory Animals as adopted and promulgated by the National Institutes of Health.

2.2. Body and lung weight and volume measurement

Animals from captopril or control group ($n = 6$ per treatment) were sacrificed by decapitation at different stages, P0, P8, P15 and P30 (2–3 per age). After that, body and lung weights were registered and lung/body ratios were estimated.

Lung volumes were determined according to the submersion method [29] in which water displaced due to organ volume is recorded by weighing (W). As the isotonic saline specific density (d) is 1.0048, the respective volumes were obtained by: V [structure] (cm^3) = W (g)/d or simply V (cm^3) = W (g).

2.3. Biochemical studies

Blood from pregnant rats was collected from G13 until G19, every two days, from the tail in tubes without anticoagulant. From each dam, pups were sacrificed by decapitation and blood obtained at P0, P8, P15 and P30. After sampling, tubes were centrifuged at 1500 ×*g* for 10 min and immediately stored at −20 °C until assay. Serum ACE measurements were performed by a direct spectrophotometric assay based on the hydrolysis of the synthetic tripeptide substrate 2-furanacryloyl-L-phenylalanylglycylglycine (FAPGG) to furanacryloylphenylalanine (FAP) and glycylglycine. Absorbance (340 nm) was measured after 3 min and 30 min incubation at 37 °C. Δ*A*/min determination and unit l^{-1} conversion was as described [30].

2.4. Reverse transcriptase-polymerase chain reaction assay

From each dam, one pup at each stage, P0, P8, P15 and P30, was sacrificed by decapitation, and lungs were harvested, weighed and immediately snap frozen on isopentane (−30 °C) and stored at −80 °C until use.

Total RNA was isolated using TRIzol reagent (Invitrogen Life Technologies) according to the manufacturer's protocols. RNA's quality was tested by measuring optical density ratios (OD_{260}/OD_{280}) of at least 1.8 and their integrity visualized with agarose gels.

Total RNA (2 μg) from lung was retro-transcribed by using M-MLV reverse transcriptase with 1 μM oligo-d(T) primer. PCR assays were performed in 20 μl final volume, containing cDNA (2 μl), 2 U of *Taq* DNA polymerase [31] using a thermocycler (ep gradient Eppendorf Mastercycler).

sACE primers (Table 1) were designed with slight modifications of those previously published [7] (GenBank ID: NM_012544). Primers for AT_1 receptor were designed using NCBI BLAST search (GenBank ID: NM_030985). Glyceraldehyde 3-phosphate dehydrogenase (GAPDH) mRNA was used as a housekeeping-gene control [32]. PCR products were analyzed by electrophoresis on 1.5% agarose gels, visualized by GelRed staining and bands quantified using Scion Image. The absence of genomic DNA contamination was confirmed by performing PCR with an equivalent amount of total RNA without reverse transcription.

Table 1
Primers and PCR thermocycling parameters.

Primer	Sequence	PCR conditions	Size (bp)	Ref.
sACE	F: 5′-TTCGTGCTACAGTTCCAG-3′ R: 5′-CTTCTTTATGATCCGCTT-3′	32 cycles: 95 °C, 45 s; 52 °C, 1 min; 72 °C, 1 min. Final extension: 72 °C, 7 min.	569	[7]
GAPDH	F: 5′-TCCCTCAAGATTGTCAGCAA-3′ R: 5′-AGATCCACAACGGATACATT-3′	32 cycles: 95 °C, 45 s; 52 °C, 1 min; 72 °C, 1 min. Final extension: 72 °C, 7 min.	309	[32]
AT_1 receptor	F: 5′-GTCATGATCCCTACCCTCTACAGC-3′ R: 5′-CCGTAGAACAGAGGGTTCAGGCAG-3′	32 cycles: 95 °C, 1 min; 64 °C, 1 min; 72 °C, 1 min. Final extension: 72 °C, 7 min.	823	

sACE: somatic angiotensin converting enzyme; GAPDH: glyceraldehyde phosphate dehydrogenase; F: forward primer; R: reverse primer.

Table 2
Lung volume and lung/body weight ratio from control and captopril-treated rats at the different postnatal stages.

	0 day	8 days	15 days	30 days
Lung volume				
Control	0.27 ± 0.02	0.35 ± 0.05	0.72 ± 0.02	0.97 ± 0.02
Captopril	0.22 ± 0.02	0.32 ± 0.02	0.65 ± 0.05	0.90 ± 0.10
Lung/body weight (%)				
Control	2.42 ± 0.21	2.66 ± 0.00	2.04 ± 0.00	1.02 ± 0.06
Captopril	1.81 ± 0.19	3.13 ± 0.39	2.86 ± 0.46	1.07 ± 0.07

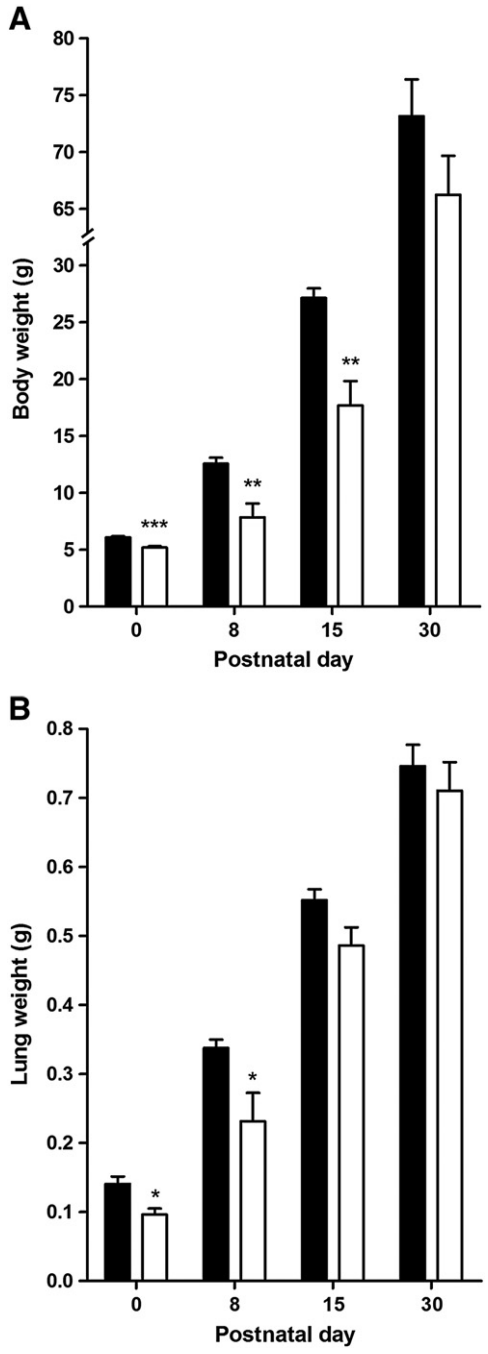

Fig. 1. Body and lung weight in control and captopril-treated rats at different postnatal ages. A) Body weight decreased significantly at P0, P8 and P15 in captopril-treated rats (**p<0.01 and ***p<0.001). B) Lung weight showed a significant decrease at P0 and P8 (*p<0.05). Data are mean ± SEM from 2 to 3 animals per age from six independent treatments ($n = 18$). ■: control; □: captopril.

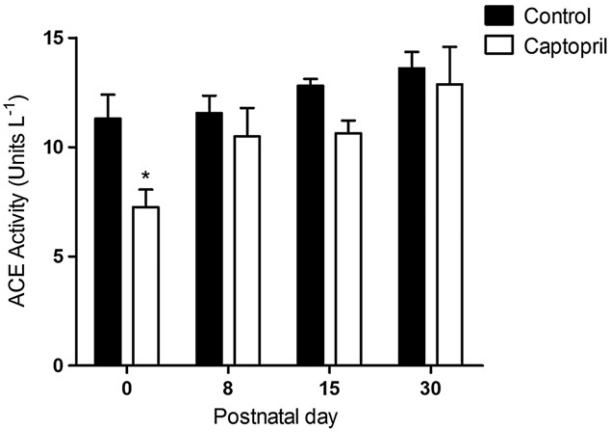

Fig. 2. Serum ACE activity in control and captopril-treated pups. Serum ACE activity was evaluated by FAPGG hydrolysis at different postnatal ages. Data are mean ± SEM from three independent treatments of the pregnant mothers, 3 animals per treatment ($n = 9$). ACE activity decreased significantly in neonatal (P0) captopril-treated rats (*p<0.05).

2.5. Western blot analysis

Lung protein extraction was performed as described [33]. Briefly, lungs were homogenized (300–500 mg of tissue) in cold RIPA buffer (10 mM Tris–HCl, pH 7.4, 150 mM NaCl, 1% Triton X-100, 0.1% SDS, and 1 mM EDTA), containing fresh protease inhibitor (2 mM PMSF). Samples were centrifuged at 10,000 ×*g* for 15 min, and the supernatant was collected and used as protein extract for immunoblotting analysis. Protein concentration was determined by Bradford, using an absorbance reader (BioTec), and compared to a BSA standard curve.

Proteins (50 μg) were subjected to SDS-PAGE and electroblotted onto nitrocellulose membrane (Millipore-P). Membranes were blocked with 3% nonfat dry milk in tris-buffered saline/0.1% Tween 20 (TBS-T).

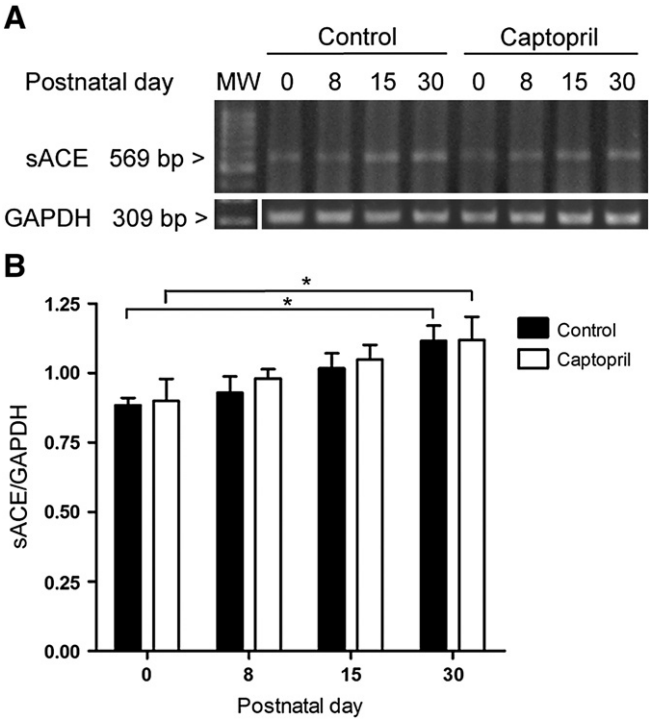

Fig. 3. Somatic ACE (sACE) expression at different postnatal ages in control and captopril-treated rat lungs. A. Representative gel from the RT-PCR products of sACE and GAPDH for control and treated groups. MW: molecular weight marker. B. Densitometric data normalized against GAPDH, shown as mean ± SEM of six independent experiments. sACE expression evidenced a significant increase from P0 to P30, in both groups (*p<0.05).

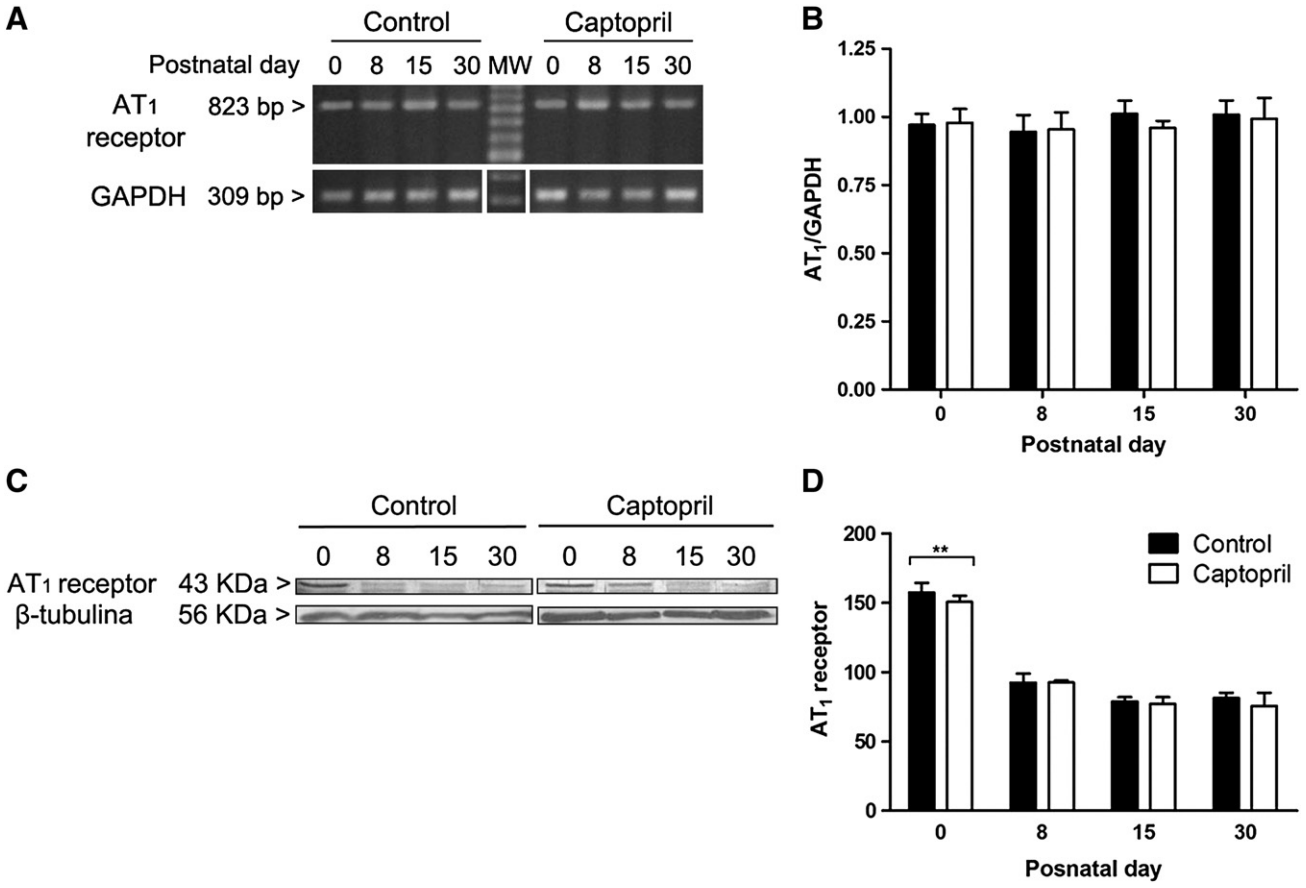

Fig. 4. AT_1 receptor expression of control and captopril-treated groups in developing lungs. A. Representative gel from the RT-PCR performed to evaluate mRNA expression of AT_1 receptor and normalized against GAPDH for different stages and treatments. MW: molecular weight marker. B. Densitometric data are shown as mean ± SEM of six independent experiments. C. Western blot analysis showing AT1 receptor protein expression in lung development; β tubulin is used as loading control. D. Data represent mean ± SEM of three independent experiments Western blot analyses normalized to Beta-tubulin.

Membranes were then incubated overnight at 4 °C with anti-AT_1 receptor primary antibody (SC-579, 1:2000) and then incubated with secondary antibody (1:10,000) coupled to HRP (Jackson ImmunoResearch). Blots were developed with ECL and membranes were reprobed for β-tubulin as loading control.

2.6. Lung processing and histological analysis

For histological analysis only male pups were considered [34]. Briefly, after sacrifice by cervical dislocation, the trachea was exposed and cannulated. Lungs were inflated by applying a constant pressure (25 cm of water) with 0.5% low melting-point agarose dissolved in 10% buffered formalin (pH 7.4), and incubated on ice to allow agarose to solidify. Left lungs were fixed in 10% buffered formalin (4 °C, overnight) and washed in phosphate-buffered saline (PBS). Fixed tissues were dehydrated in ascending series of ethanol, cleared in xylene and stained with hematoxylin–eosin (H&E). As lung maturation varies along different regions of developing lung, all studies were performed on the distal portion of the left lobe.

2.7. Measurement of mean linear intercept

The degree of alveolar septation in male pups was estimated by mean linear intercept (MLI) measurements, as described previously [22,23]. Briefly, eight random lung sections per animal were viewed at 40× magnification and a superimposed predetermined grid (1 mm). The line that crossed a large vessel or bronchus was excluded from evaluation. Points at which an alveolar septum intercepted a line were counted separately. The total length of all lines counted was divided by the total number of intercepts per field examined. MLI, which is inversely proportional to alveolar surface area, was expressed in micrometers (μm). Images were acquired using a microscope (Nikon Eclipse 50i).

2.8. Immunostaining

Immunohistochemistry for PCNA and α-SMA was performed as described [35]. Sections (5 μm) from fixed tissues were mounted on slides treated with 3-aminopropyltriethoxysilane (Sigma-Aldrich, St. Louis, MO, USA). After deparaffinization, sections were pre-treated for antigen retrieval with 0.01 M citrate buffer (pH 6.0) and microwave. Endogen peroxidase activity was inhibited with 1% H_2O_2 and nonspecific binding blocked with 10% (v/v) normal goat serum. Lung sections were incubated with a mouse monoclonal antibody to PCNA (1:200; Santa Cruz Biotechnology, SC-56) or mouse monoclonal antibody to α-SMA (1:50; Novocastra-NCL-SMA) for 18 h at 4 °C and then with anti-mouse biotinylated secondary antibody (30 min, room temperature). Antigens were visualized by streptavidin-peroxidase

Fig. 5. Airway morphology and morphometric measurements of lung sections in postnatal development. A. Representative photomicrograph of control (a, c, e, g) and captopril-treated (b, d, f, h) groups at P0, P8, P15 and P30. Larger airway spaces can be observed in captopril-treated lungs (asterisks). Scale bars = 100 μm. B. Morphometric quantification of alveolar sizes by mean linear intercept (MLI) from control and captopril-treated groups during development. Captopril-treated animals showed significative differences at P8, P15 (***$p<0.001$) and P30 (*$p<0.05$) compared with control. In control animals, P0 was significantly different from all other stages (**$p<0.01$). Data are mean ± SEM, from six independent treatments.

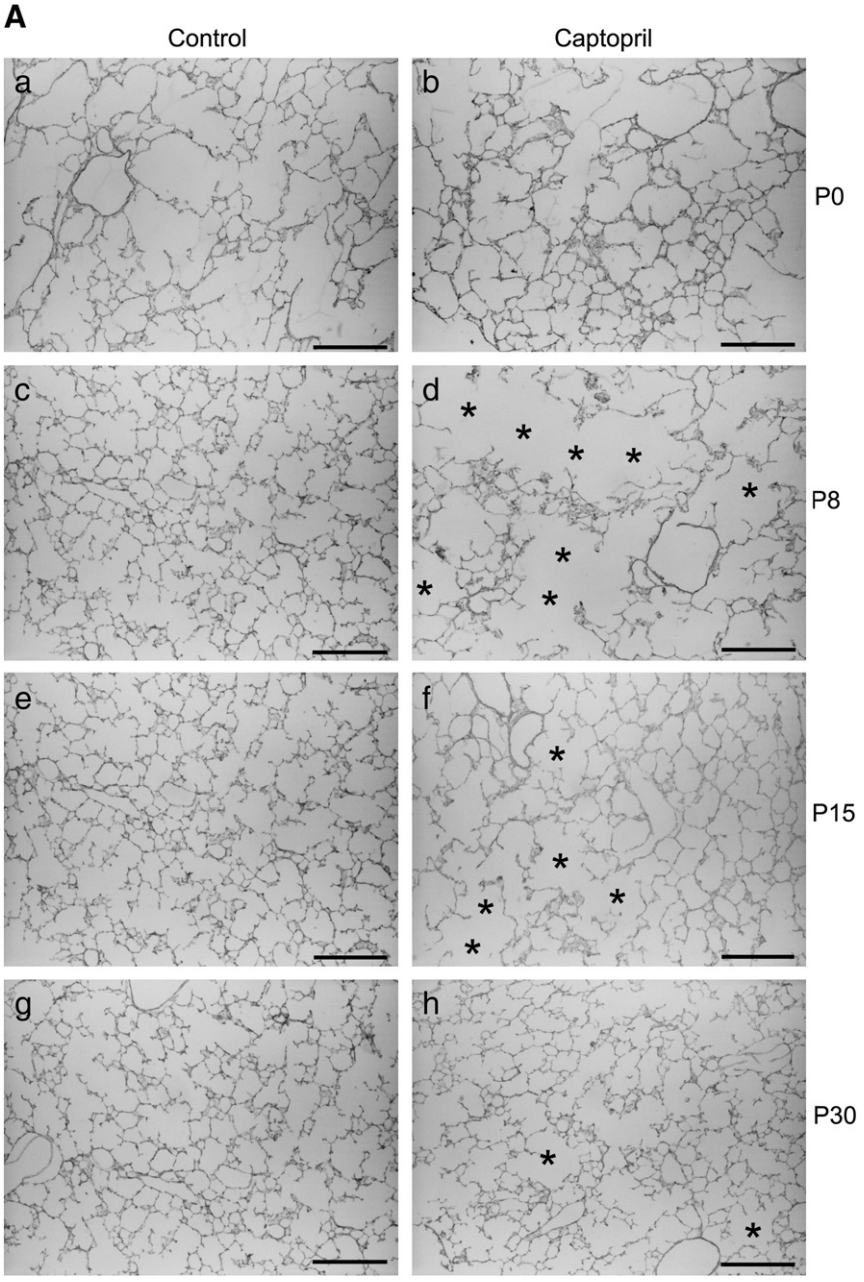
A
Control
Captopril
a
b
P0
c
d
P8
e
f
P15
g
h
P30

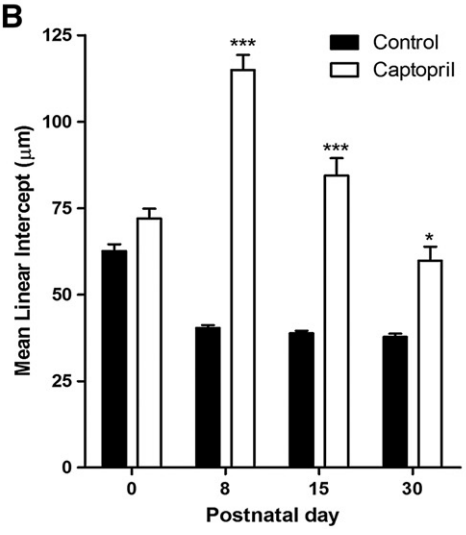
B
Control
Captopril
Mean Linear Intercept (μm)
125
100
75
50
25
0
***
***
*
0
8
15
30
Postnatal day

(BioGenex, San Ramon, CA) and 3.3-diaminobenzidine chromogen (Liquid DAB-Plus Substrate Kit-Zymed, San Francisco, CA) was used. The slides were counterstained with hematoxylin. A minimum of 1000 alveolar cells per sample were counted, and PCNA immunopositive cells were expressed as a percentage. The number of α-SMA stained myofibroblasts at the tips of developing septa was counted in 10 fields per lung and 3 lungs per age and treatments were analyzed at 400× magnification. Sections at the distal portion of the left lung were analyzed in control and captopril-treated animals.

For co-localization, lung sections were first incubated with mouse monoclonal antibody to PCNA for 1 h at 25 °C, followed with anti-mouse biotinylated secondary antibody (30 min, 25 °C) and visualized by streptavidin-peroxidase (brown). After that, sections were stained with anti-cytokeratin (Zimed) mouse monoclonal antibody (1:500), incubated at 4 °C overnight and then with anti-mouse biotinylated secondary antibody (30 min, 25 °C). Antigens were visualized with amino ethyl carbazol (red) (AEC, Biogenex HK 330-9K).

2.9. Statistical analysis

Data are expressed as mean ± SEM. Statistical analysis was done using Student's *t*-test for two groups. Statistical differences among groups were compared with One-way Analysis of Variance (ANOVA) followed by Tukey–Kramer's Multiple Comparison Test (GraphPad Prism 5). Statistical significance was accepted with probability value of $p<0.05$.

3. Results

3.1. Body and lung weights and volume

Pregnant rats were treated during the last week of pregnancy with either, the ACE inhibitor captopril ($n=6$) or saline solution as control ($n=6$). Litter sizes were comparable in both groups; control (12–14) and captopril (11–13). From each mother, 2–3 pups per age were weighted (Fig. 1A). Body weight was significantly lower at P0 ($p<0.001$), P8 and P15 ($p<0.01$) in captopril-treated rats, compared to control animals. Similarly, the lung weight of male pups at P0 and P8 was lower in captopril-treated rats compared to the control group ($p<0.05$) (Fig. 1B). Comparison of the lung/body weight ratios and lung volume showed no statistically significant differences between captopril-treated and control groups at the different ages studied (Table 2). Moreover, captopril administration during late pregnancy induced a high mortality rate during the first postnatal week. Pups died spontaneously (21.6%, $p<0.05$), after birth and before P8 in the captopril group, while no one died in the control group over the same period.

3.2. Biochemical and molecular analyses of the renin–angiotensin system

To evaluate whether treatment with captopril was accompanied by serum ACE inhibition, we determined ACE activity in serum from pregnant rats and offspring at different times. No significant differences were observed in serum ACE activity in treated pregnant rats, with respect to the control (data not shown). On the contrary, a significant decrease in ACE activity was observed in P0 pups born from captopril-treated mothers (Fig. 2). No significant differences were observed in P8, P15 and P30 pups.

sACE expression during lung development was evaluated by RT-PCR in control and captopril-treated groups (Fig. 3). sACE expression level increased with lung development in both treated and control groups.

In addition, we evaluated the effect of ACE inhibition on AT_1 receptor expression by RT-PCR at different postnatal ages (Fig. 4). AT_1 receptor expression did not vary in lungs from P0 to P30 in control and treated animals. On the other hand, AT_2 receptors were not detectable by RT-PCR in control and captopril-treated animals at the different ages studied (data not shown). Protein levels of Ang II AT_1 receptor were determined by Western blot (Fig. 4C). The level of AT_1 receptor is higher in P0 pups and drops after that. However, no differences were observed in both the control and treated groups (Fig. 4D).

3.3. Histological analysis

Following treatment with captopril, lung development was evaluated by histological analysis in distal parenchyma from control and treated animals at different ages. To exclude the possibility of variation due to sex [34], just male pups were considered for histological evaluation.

Fig. 5 shows the typical architecture in control lungs at P0, P8, P15 and P30 stained with H&E (a, c, e and g, respectively). Lung tissue sections from the captopril-treated group (b, d, f, h) showed morphologic changes in the lung architecture, particularly at P8 and P15 (Fig. 5d and f). Lungs from the captopril-treated group showed impaired alveolar formation, resulting in enlargement of distal airway spaces at P8, P15 and P30. The interalveolar wall distance measured by MLI was increased for the treated group vs. age-matched controls at P8 and P15 ($p<0.001$) and a tendency to recover was observed at P30 ($p<0.05$) (Fig. 5B). The morphological changes observed such as increased airway spaces and delayed septation, resemble the typical cytoarchitecture observed in new BPD [26].

3.4. Immunolocalization of PCNA

PCNA antigen is a well-known marker of cellular proliferation. Since cellular proliferation is a necessary mechanism in the process of alveolarization for the postnatal lung development, we evaluated PCNA immunolocalization in distal lung sections from both groups at the different stages studied.

Fig. 6 shows microscopic images from control lungs (a, c, e and g) and the treated ones (b, d, f and h) at P0, P8, P15 and P30 stages. The PCNA marker localized mainly at the nucleus of pneumocyte cells (see Fig. 6, inset), identified by co-immunostaining (see Fig. S1). The percentage of PCNA-positively stained alveolar epithelial cells in the treated group was significantly higher at P15 and P30 than in the control group (Fig. 6B). Cell proliferation in control animals decreased significantly during the postnatal stages studied ($p<0.001$), while in captopril-treated lungs the relative number of PCNA immunopositive nuclei remains high along the same period.

3.5. Immunolocalization of α-SMA

Smooth muscle actin (α-SMA) is a molecular marker of interstitial myofibroblasts, during septal formation [36]. Localization of α-SMA by immunohistochemistry was evaluated in control and treated lungs at different postnatal stages. In animals born from captopril-treated mothers, at P8 and P15, α-SMA staining was prevalent at the tips of the developing secondary septa (Fig. 7). Most of these cells are presumed to be myofibroblasts, especially active in elastogenesis and septal elongation during postnatal development [23,36]. The number of developing tips per field was higher at P15 in those animals born from mothers treated with captopril than in control animals (3.83 ± 0.26 vs. 2.5 ± 0.22, $p<0.05$). Fig. 7e shows α-SMA immunostaining present in the smooth muscle of bronchial, bronchiolar and vessel walls in P15 control animals.

4. Discussion

The intrapulmonary renin–angiotensin system has been demonstrated during fetal development and suggests multiple effects on pulmonary physiology [12,27]. Knock-out animals for ACE, Ang II

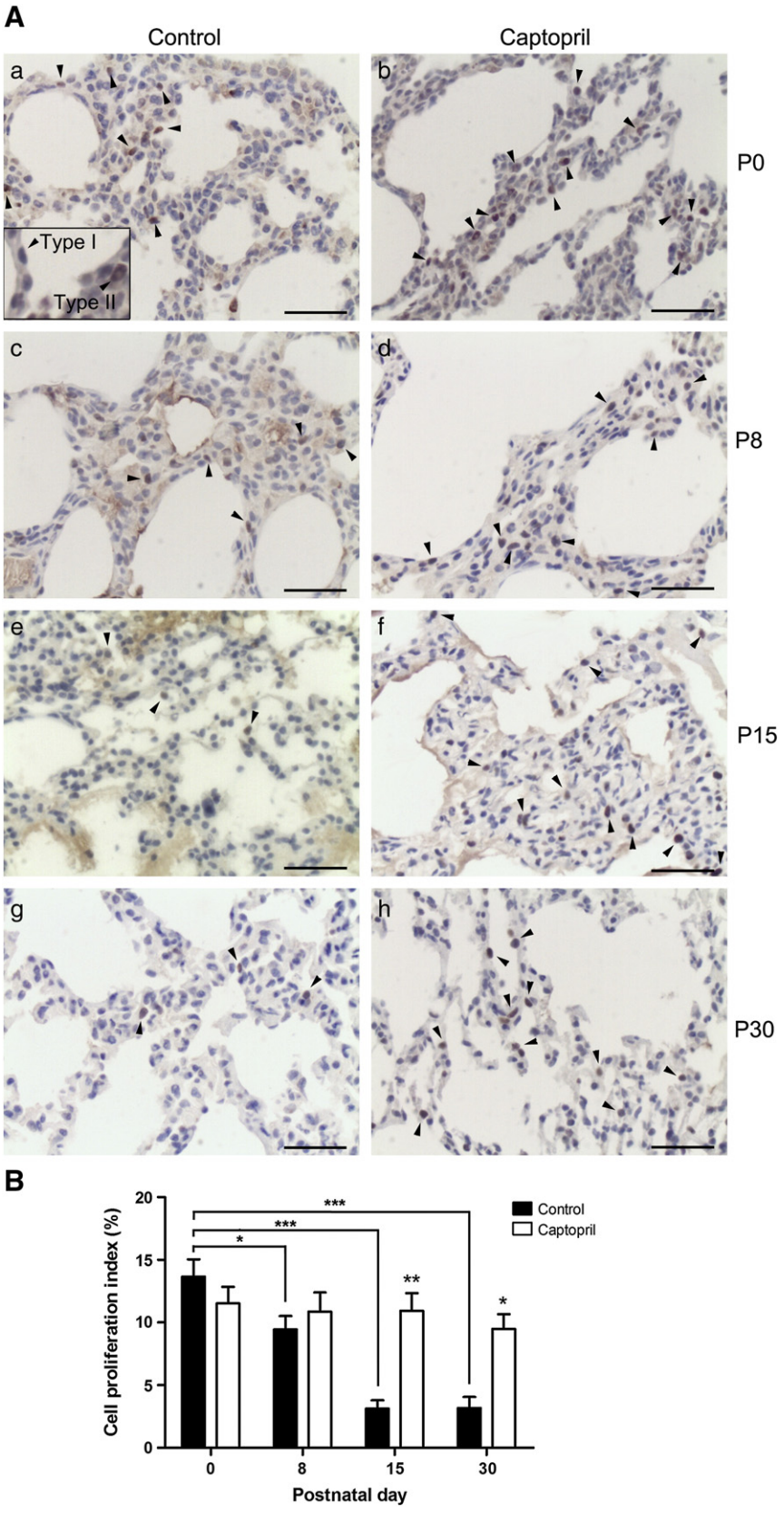

Fig. 6. Immunolocalization of proliferating cell nuclear antigen (PCNA) in postnatal lung development. A. Immunohistochemistry of PCNA (brown) counterstained with hematoxylin. Positive staining (arrowheads) for PCNA was observed in the alveolar septa in control lungs (a, c, e, g) and captopril-treated lungs (b, d, f, h) at P0, P8, P15 and P30. Scale bars = 20 μm. B. Positive cells were quantified and data expressed as a percentage of total pneumocytes. PCNA-positive cells, observed in epithelial airways were higher at P15 (**$p<0.01$) and P30 (*$p<0.05$) in captopril-treated lungs than in control. Cell proliferation in control animals decreased significantly during the postnatal period, (P0 vs. P8; *$p<0.05$, P0 vs. P15 and P30; ***$p<0.001$). Data are mean ± SEM from three independent treatments.

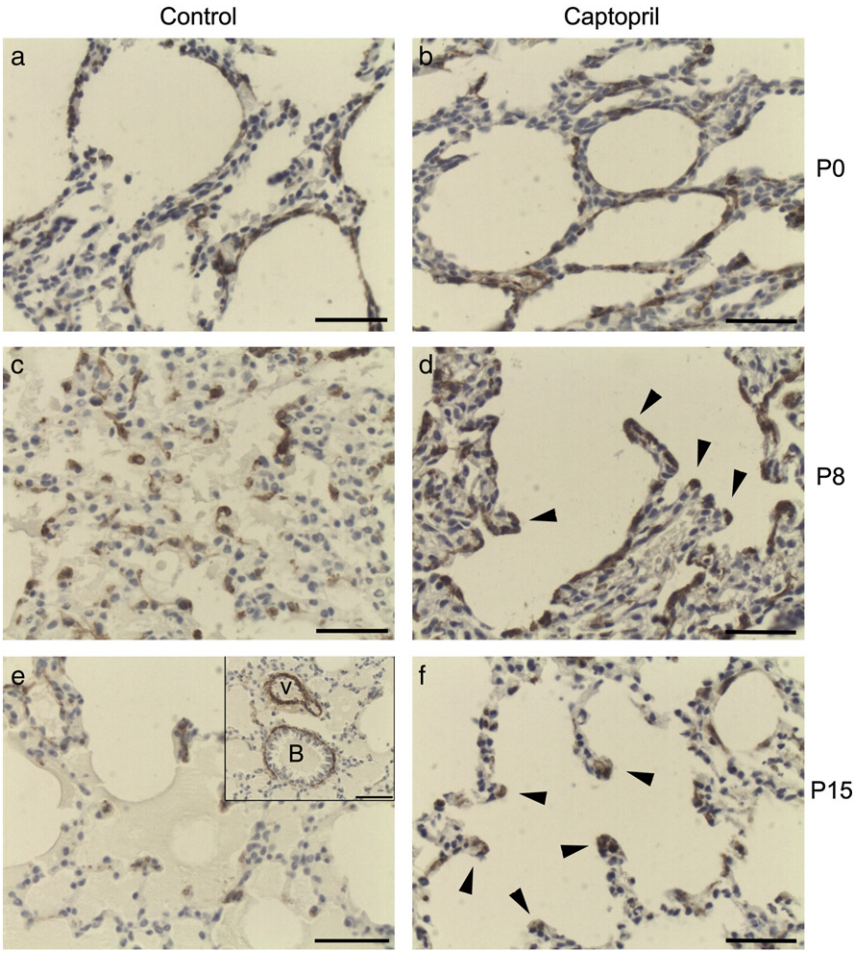

Fig. 7. Immunolocalization of α-smooth muscle actin (α-SMA) during developing lung in control (a, c, e) and captopril-treated (b, d, f) animals. α-SMA recognized myofibroblasts at the tips of developing septa (*arrowhead*) or smooth muscle cells at bronchiolar (B) and vessel (V) walls (e, *upper panel*). Bars = 20 μm.

AT_1 receptors or angiotensinogen evidenced similar effects, such as blood pressure reduction, renal dysfunction and male infertility [13]. ACE inhibitors can be teratogenic in human embryos [9,10,18,19,37], while in animals, RAS inhibition causes fetopathies and renal anomalies after birth [3,4,8]. However, detailed evaluation of lung malformation in either knock-out mice or animals treated with ACE inhibitors remains unexplored. In the present study, we examined the effects of maternal exposure to captopril during late pregnancy (G13–G21) on postnatal lung development in rats. Our present results evidenced lung and body weight alterations, serious lung histomorphological damage, comparable to new BPD and altered expression of PCNA and α-SMA in lung development, following prenatal treatment with captopril.

The lower lung and body weight observed at initial postnatal stages could be a consequence of captopril in lung development directly through the RAS or secondary to oligohydramnios [8], which is known to retard lung cell differentiation in rats. Kitterman et al. reported a reduction of the number of type I pneumocytes in experimental oligohydramnios [38].

In the present study we used a dose of captopril comparable to the one used by Martinez et al. [39], and considerably lower than the one used by other authors [40,41]. We choose a dose which did not lower the blood pressure of the mother to avoid indirect effects. Treatment had no effect in serum ACE activity of pregnant rats but a significant decrease in ACE activity was observed in P0 pups. Taking into account that pregnant rats are resistant to alterations in Ang II concentration [42], the lack of effect of captopril-treatment in mothers suggests that the observed effect in pups is not caused by a significant decreased in Ang II levels in the pregnant rat. Since ACE inhibitors increase bradykinin levels and stimulate prostaglandin release, both might contribute to the pharmacological effects of ACE inhibitors [8]. However, we observed a significant decrease on ACE activity in P0 animals, thus confirming transplacental transfer of captopril as reported earlier [10,17,18]. Since treatment was stopped after birth, we did not expect changes in serum ACE activity later on during development (P8, P15, P30).

The existence of a local pulmonary RAS and high level of pulmonary ACE, prompted us to investigate the expression of RAS components. The expression level of sACE increased with age in developing lungs from control as well as captopril-treated animals, showing no difference between both groups. Our present observations are in accordance with previous data which report increased ACE activity during lung development [2,27,28].

Early studies in vascular smooth muscle cells pointed-out that treatment with Ang II down-regulates AT_1 receptor expression [43]. Studies by in situ hybridization showed that AT_{1A} receptors are continuously expressed in the lung parenchyma from E19 to P3 [44]. Decrease in serum ACE activity observed in P0 pups could lower Ang II circulating levels. Thus, we explored the expression level of both Ang II receptor subtypes at different postnatal ages following treatment. AT_1 receptor expression was high and maintained in lungs from control pups and those exposed to captopril during late pregnancy suggesting an important role of this receptor during lung development. On the contrary, AT_2 receptors were not detectable by RT-PCR in control or treated animals at the different ages studied, which is in agreement with previous reports [44,45]. However, the

presence of AT_2 receptors has been reported in fetal stages in bronchial epithelial cells [12]. When protein levels of AT_1 receptors were compared, no differences were observed between treatments. However, the protein level was considerably higher in P0 animals, thus suggesting a post-translational regulation.

In human, new BPD occurs postnatally either in very low birth weight premature neonates or as a consequence of multiple factors: immaturity, perinatal infection and inflammation, persistent ductus arteriosus and disrupted alveolar and capillary development [25,26]. New BPD is characterized by deficit in alveolar number and increased airspace size, leading to reduction of the exchange-surface-to-volume ratio and respiratory insufficiency.

The major finding of our study was a clear adverse effect of prenatal treatment (G13–G21) with captopril on the postnatal lung histomorphology that closely resembles new BPD in premature newborns. Histomorphological changes were also observed in a postnatal treatment with enalapril at a higher dose [24].

At the dose used in this study, significant changes in the histoarchitecture were observed at the stages P8, P15 and P30. At birth, rat lungs are at early stage of development, named as saccular stage. Due to the preliminary level of development achieved by the lungs at rat birth, no major differences between treatments were observed at this stage (P0). During the first postnatal weeks, lung development is critical in order to increase the air–blood exchange surface. Treatment might cause a delay in cellular proliferation at the saccular stage of lung development, leading to the enlarged airspaces observed at P8, P15 and P30 lungs in comparison with control animals. Thus, treatment could affect the process of secondary septa formation. However, the cells kept their growth capacity which allows a recovery after that.

Since lung development is mainly postnatal in rodents, cellular proliferation is expected during the active alveoli septation process. In control animals, the PCNA cellular proliferation marker was higher at P0 and then drops gradually. On the contrary, in animals treated with captopril, the PCNA marker remains at higher levels at all stages studied. Since PCNA expression in the treated group was maintained, we can speculate that proliferation of epithelial cells occurs as part of a healing process to complete alveolarization, following the BPD-like damage induced by captopril treatment. Besides, α-SMA was prevalent at the tips of developing secondary septa in the enlarged airway spaces observed in captopril-treated lungs at P8 and P15. Myofibroblasts expressing α-SMA are associated with regions and periods of development and remodeling [36,46,47] as well as in injury repair [47]. In addition, the role of Ang II as a promoter of human lung fibroblast cell differentiation into myofibroblasts and increased collagen production has been shown [48]. Thus, α-SMA localization in the treated group reinforces the increased expression of PCNA, suggesting an essential participation in the secondary septation that forms the alveoli during lung maturation.

In summary, prenatal treatment with captopril at the dose used impairs lung alveolarization at postnatal stages. Taking into account that in rodents lungs at birth are immature and development completes postnatally, the histomorphological effects produced by ACE inhibition during late pregnancy suggest participation of the RAS during lung alveolarization. Our present observations suggest that beyond the damage caused by the use of captopril during late pregnancy, cells of the developing lungs kept their ability to proliferate and recover.

Supplementary data to this article can be found online at http://dx.doi.org/10.1016/j.regpep.2012.05.092.

Acknowledgments

We wish to thank MR Marini and AL Sacrtascini Ciorciari from the Laboratory of Cito-Histopathology (FCV-UNL) for histopathologic analysis contributions. We also thank members of the Laboratory of Cellular Biology (FCV-UNL) for their technical support. GM Ciuffo and HH Ortega are members of the researcher's career of CONICET. DN Capelari has fellowships from CONICET. This work was supported by grants from CONICET, PICT15-32350 (ANPCYT) and UNSL, Argentina.

References

[1] de Gasparo M, Catt KJ, Inagami T, Wright JW, Unger T. International union of pharmacology. XXIII. The angiotensin II receptors. Pharmacol Rev 2000;52:415–72.
[2] Tufro-McReddie A, Gomez RA. Ontogeny of the renin–angiotensin system. Semin Nephrol 1993;13:519–30.
[3] Lasaitiene D, Chen Y, Adams MA, Friberg P. Further insights into the role of angiotensin II in kidney development. Clin Physiol Funct Imaging 2006;26:197–204.
[4] Sanchez SI, Seltzer AM, Fuentes LB, Forneris ML, Ciuffo GM. Inhibition of angiotensin II receptors during pregnancy induces malformations in developing rat kidney. Eur J Pharmacol 2008;588:114–23.
[5] Sanchez SI, Arce ME, Fuentes LB, Ciuffo GM. Prenatal blockade of Ang II receptors affects neonatal rat hindbrain structure and receptor localization. Exp Neurol 2009;220(2):246–54.
[6] Corvol P, Williams TA, Soubrier F. Peptidyl dipeptidase A: angiotensin I-converting enzyme. Methods Enzymol 1995;248:283–305.
[7] Tian XL, Paul M. Species-specific splicing and expression of angiotensin converting enzyme. Biochem Pharmacol 2003;66:1037–44.
[8] Buttar HS. An overview of the influence of ACE inhibitors on fetal-placental circulation and perinatal development. Mol Cell Biochem 1997;176:61–71.
[9] Pryde PG, Sedman AB, Nugent CE, Barr Jr M. Angiotensin-converting enzyme inhibitor fetopathy. J Am Soc Nephrol 1993;3:1575–82.
[10] Quan A. Fetopathy associated with exposure to angiotensin converting enzyme inhibitors and angiotensin receptor antagonists. Early Hum Dev 2006;82:23–8.
[11] Cox RM, Anderson JM, Cox P. Defective embryogenesis with angiotensin II receptor antagonists in pregnancy. BJOG 2003;110:1038.
[12] Nogueira-Silva C, Carvalho-Dias E, Piairo P, Nunes S, Baptista MJ, Moura RS, Correia-Pinto J. Local fetal lung renin–angiotensin system as a target to treat congenital diaphragmatic hernia. Mol Med 2011;18(1):231–43.
[13] Bernstein KE. Views of the renin–angiotensin system: brilling, mimsy, and slithy tove. Hypertension 2006;47:509–14.
[14] Kaparianos A, Argyropoulou E. Local renin–angiotensin II systems, angiotensin-converting enzyme and its homologue ACE2: their potential role in the pathogenesis of chronic obstructive pulmonary diseases, pulmonary hypertension and acute respiratory distress syndrome. Curr Med Chem 2011;18:3506–15.
[15] Marshall RP, Webb S, Bellingan GJ, Montgomery HE, Chaudhari B, McAnulty RJ, Humphries SE, Hill MR, Laurent GJ. Angiotensin converting enzyme insertion/deletion polymorphism is associated with susceptibility and outcome in acute respiratory distress syndrome. Am J Respir Crit Care Med 2002;166:646–50.
[16] Yamazato Y, Ferreira AJ, Hong KH, Sriramula S, Francis J, Yamazato M, Yuan L, Bradford CN, Shenoy V, Oh SP, Katovich MJ, Raizada MK. Prevention of pulmonary hypertension by angiotensin-converting enzyme 2 gene transfer. Hypertension 2009;54:365–71.
[17] Stevenson KM, Gibson KJ, Lumbers ER. Comparison of the transplacental transfer of enalapril, captopril and losartan in sheep. Br J Pharmacol 1995;114:1495–501.
[18] Cooper WO. Clinical implications of increased congenital malformations after first trimester exposures to angiotensin-converting enzyme inhibitors. J Cardiovasc Nurs 2008;23:20–4.
[19] Tabacova S, Little R, Tsong Y, Vega A, Kimmel CA. Adverse pregnancy outcomes associated with maternal enalapril antihypertensive treatment. Pharmacoepidemiol Drug Saf 2003;12:633–46.
[20] Metzger RJ, Klein OD, Martin GR, Krasnow MA. The branching programme of mouse lung development. Nature 2008;453:745–50.
[21] Burri PH. Structural aspects of prenatal and postnatal development and growth of the lung; 1997.
[22] Chen H, Zhuang F, Liu YH, Xu B, Del Moral P, Deng W, Chai Y, Kolb M, Gauldie J, Warburton D, Moses HL, Shi W. TGF-beta receptor II in epithelia versus mesenchyme plays distinct roles in the developing lung. Eur Respir J 2008;32:285–95.
[23] Pua ZJ, Stonestreet BS, Cullen A, Shahsafaei A, Sadowska GB, Sunday ME. Histochemical analyses of altered fetal lung development following single vs multiple courses of antenatal steroids. J Histochem Cytochem 2005;53:1469–79.
[24] Lasaitiene D, Chen Y, Nannmark U, Wollmer P, Friberg P. Neonatal ACE inhibition in rats interferes with lung development. Clin Physiol Funct Imaging 2004;24:65–8.
[25] Bourbon JR, Boucherat O, Boczkowski J, Crestani B, Delacourt C. Bronchopulmonary dysplasia and emphysema: in search of common therapeutic targets. Trends Mol Med 2009;15:169–79.
[26] Bancalari E, Claure N, Sosenko IR. Bronchopulmonary dysplasia: changes in pathogenesis, epidemiology and definition. Semin Neonatol 2003;8:63–71.
[27] Morrell NW, Grieshaber SS, Danilov SM, Majack RA, Stenmark KR. Developmental regulation of angiotensin converting enzyme and angiotensin type 1 receptor in the rat pulmonary circulation. Am J Respir Cell Mol Biol 1996;14:526–37.
[28] Powell JT, Whitney PL. Postnatal development of rat lung. Changes in lung lectin, elastin, acetylcholinesterase and other enzymes. Biochem J 1980;188:1–8.
[29] Scherle W. A simple method for volumetry of organs in quantitative stereology. Mikroskopie 1970;26:57–60.
[30] Murray BA, Walsh DJ, FitzGerald RJ. Modification of the furanacryloyl-L-phenylalanylglycylglycine assay for determination of angiotensin-I-converting enzyme inhibitory activity. J Biochem Biophys Methods 2004;59:127–37.
[31] Manzur MJ, Muñoz R, Lucero AA, Juri Ayub M, Alvarez SE, Ciuffo GM. Production of recombinant enzymes of wide use for research. Electron J Biotechnol 2006.

[32] Terada Y, Tomita K, Nonoguchi H, Marumo F. PCR localization of angiotensin II receptor and angiotensinogen mRNAs in rat kidney. Kidney Int 1993;43:1251–9.
[33] Ruest LB, Khalyfa A, Wang E. Development-dependent disappearance of caspase-3 in skeletal muscle is post-transcriptionally regulated. J Cell Biochem 2002;86:21–8.
[34] Adamson IY, King GM. Sex differences in development of fetal rat lung. II. Quantitative morphology of epithelial–mesenchymal interactions. Lab Investig 1984;50: 461–8.
[35] Ortega HH, Salvetti NR, Padmanabhan V. Developmental programming: prenatal androgen excess disrupts ovarian steroid receptor balance. Reproduction 2009;137: 865–77.
[36] Yamada M, Kurihara H, Kinoshita K, Sakai T. Temporal expression of alpha-smooth muscle actin and drebrin in septal interstitial cells during alveolar maturation. J Histochem Cytochem 2005;53:735–44.
[37] Guron G, Molne J, Swerkersson S, Friberg P, Hansson S. A 14-year-old girl with renal abnormalities after brief intrauterine exposure to enalapril during late gestation. Nephrol Dial Transplant 2006;21:522–5.
[38] Kitterman JA, Chapin CJ, Vanderbilt JN, Porta NF, Scavo LM, Dobbs LG, Ertsey R, Goerke J. Effects of oligohydramnios on lung growth and maturation in the fetal rat. Am J Physiol Lung Cell Mol Physiol 2002;282:431–9.
[39] Martinez LA, Villalobos-Molina R. Early and chronic captopril or losartan therapy reduces infarct size and avoids congestive heart failure after myocardial infarction in rats. Arch Med Res 2003;34:357–61.
[40] Jugdutt BI. Effect of captopril and enalapril on left ventricular geometry, function and collagen during healing after anterior and inferior myocardial infarction in a dog model. J Am Coll Cardiol 1995;25:1718–25.
[41] Mecawi AS, Araujo IG, Fonseca FV, Almeida-Pereira G, Cortes WS, Rocha FF, Reis LC. Behavioural changes induced by angiotensin-converting enzyme inhibition during pregnancy and lactation in adult offspring rats. Clin Exp Pharmacol Physiol 2009;36:495–500.
[42] Takeda-Matsubara Y, Iwai M, Cui TX, Shiuchi T, Liu HW, Okumura M, Ito M, Horiuchi M. Roles of angiotensin type 1 and 2 receptors in pregnancy-associated blood pressure change. Am J Hypertens 2004;17:684–9.
[43] Lassegue B, Alexander RW, Nickenig G, Clark M, Murphy TJ, Griendling KK. Angiotensin II down-regulates the vascular smooth muscle AT1 receptor by transcriptional and post-transcriptional mechanisms: evidence for homologous and heterologous regulation. Mol Pharmacol 1995;48:601–9.
[44] Shanmugam S, Corvol P, Gasc JM. Angiotensin II type 2 receptor mRNA expression in the developing cardiopulmonary system of the rat. Hypertension 1996;28: 91–7.
[45] Rosenfeld CR, Zagariya AM, Liu XT, Willis BC, Fluharty S, Vidyasagar D. Meconium increases type 1 angiotensin II receptor expression and alveolar cell death. Pediatr Res 2008;63:251–6.
[46] Mitchell JJ, Reynolds SE, Leslie KO, Low RB, Woodcock-Mitchell J. Smooth muscle cell markers in developing rat lung. Am J Respir Cell Mol Biol 1990;3:515–23.
[47] Rishikof DC, Lucey EC, Kuang PP, Snider GL, Goldstein RH. Induction of the myofibroblast phenotype following elastolytic injury to mouse lung. Histochem Cell Biol 2006;125:527–34.
[48] Long X, Xiong SD, Xiong WN, Xu YJ, Zhang ZX, Cao Y, Chen J, Xu XH. Losartan inhibited angiotensin induced human lung fibroblast transformation and collagen synthesis. Zhonghua Jie He He Hu Xi Za Zhi 2007;30(4):273–8.